Proceedings of Ninth World Conference on Earthquake Engineering
August 2-9, 1988, Tokyo-Kyoto, JAPAN (Vol.II)

3-6-7

SIMULATION OF THE FAULT RUPTURE PROCESS AND NEAR FIELD GROUND MOTION BY THE THREE-DIMENSIONAL FINITE ELEMENT METHOD

Kenzo Toki[1] and Sumio Sawada[2]

[1]Disaster Prevention Research Institute, Kyoto University, Gokasho, Uji, Kyoto 611, Japan
[2]Geo Research Institute, Osaka, 1-8-4, Utsubo-honmachi, Nishi-ku, Osaka 550, Japan

SUMMARY

We show that the finite element method is a promising tool with which to analyze the fault rupture process and near-field ground motion. In our method, only the stress drop and yielding stress of the fault considered are assumed. Rupture begins at some point on the fault, at which the mobilized shear stress reaches the value of the yielding stress then is transmitted successively along the fault plane. We have developed a numerical technique that is applicable to the three-dimensional finite element method. This technique enables us to analyze a model that has a degree of freedom larger than 60,000. We simulated the rupture process of the 1971 San Fernando earthquake. To show the usefulness of our method, we compared the results of our three-dimensional simulation with the actual strong motion accelerograms obtained at two stations in the near field.

INTRODUCTION

We (Ref.1) developed a computer program with which to investigate dynamic nonlinear soil-structure interaction problems during strong earthquake ground motion. It uses a joint element to represent the contact surface between the soil and a structure such as a building or bridge. We (Ref.2) also used this method to analyze the dynamic fault process because rupture of a fault is a kind of sliding of rock blocks in contact. In this type of analysis, only the spatial distribution of the stress drop and the yield stress on the fault are necessary. The initial stress distribution is calculated by static analysis, which reflects the physical properties of the crust. In this approach, the source of the successive rupture of a fault is the strain energy released by the stress drop. Although this analysis was two dimensional, the rapid growth of computer technology, particularly the speed of calculation, has now made three-dimensional analysis possible. We therefore have developed a computation technique that saves both computer memory and CPU time, and it is now possible to simulate the fault rupture process with an F.E.M. model that has a degree of freedom larger than sixty thousand.

METHOD OF SIMULATION

In our analysis, the equation of motion at time step n is written.

$$[M]\{\ddot{u}_n\} + [C]\{\dot{u}_n\} + [K]\{u_n\} = \{f_n\} \qquad (1)$$

in which [M] is the mass, [C] the damping and [K] the stiffness matrices of the system. Newmark's β method ($\beta = 1/4$) is used in this marching algorithm. The load transfer method is used to solve the nonlinear equation of motion, in which the stiffness matrix is kept constant throughout the analysis (Ref.2). $\{f_n\}$ being the external force vector calculated from the constitutive relation of the joint elements(Ref.2). The lumped mass system is used in order to have only diagonal components in the mass matrix, which greatly saves computer memory. We also set up three conditions for the stiffness [K] and damping [C] matrices to save the memory of the computer when we established our finite element model.

(1) Rayleigh damping is assumed, the same damping factor being assigned for an entire region.
(2) The element used is a hexahedron with 8 nodal points.
(3) The element is systematically allocated like a lattice.

By condition (1), no memory need be used for the damping matrix [C]. By virtue of conditions (2) and (3), one node is connected to 8 elements in this model; therefore, it is related to the motion of 27 nodes; 81 degrees of freedom (including itself). But, the stiffness matrix is symmetric; therefore, 42 degrees of freedom are sufficient to describe the relative motion of a node. The size of the stiffness matrix thus becomes only 42 based on the number of nodes in the model. In addition, the index matrix, which defines the relation between an element of the stiffness matrix and a nodal point, is rendered unnecessary by virtue of the condition (3).

The Conjugate Gradient Method also is used in the matrix computation to save CPU time, which algorithm is suitable for a vector processor. The number of iterations thus could be fixed at 8. As only the diagonal mass element exists in the matrix, the number of iterations, 8, is large enough to get good convergence in computation.

The fault plane, modeled by a three-dimensional joint elements. The constitutive relation that represents the relation between the shear stress and deformation is shown in Fig.1. When the calculated stress, τ is less than the yield strength, τ_y , the stress-deformation relation is linear with the joint stiffness, K_{rs}. Sliding takes place if the mobilized shear stress reaches the yielding stress τ_y . A dynamic stress drop $\Delta\tau_d$, then occurs (Fig.1), and the shear stress becomes the residual strength, τ_r . A stress drop, $\Delta\tau$ is defined as $\Delta\tau = \tau_0 - \tau_r$, in which τ_0 is the initial stress. In a finite element analysis of the seismic behavior of ground, the region is truncated and eventually the reflection of seismic waves at the boundaries is induced. To avoid this, we adopted a viscous boundary.

The fault rupture process was simulated as follows: In the first stage, the initial stress produced by the tectonic force was computed by static analysis. This tectonic force was applied uniformly at both lateral ends to simulate the tectonic force which was increased gradually until the mobilized shear stress of a joint element on the fault plane reached the yield strength of that element. In the second stage of dynamic analysis, the mobilized stress of an element on the fault plane coincided with the yield strength of that element, therefore rupture took place immediately. Thus the strain energy of the element was released and was the origin of the fault rupture. That is, the external force vector $\{f_1\}$ in the first iteration in equation (1) is the nodal force equivalent to the dynamic stress drop of the joint element corresponding to the origin.

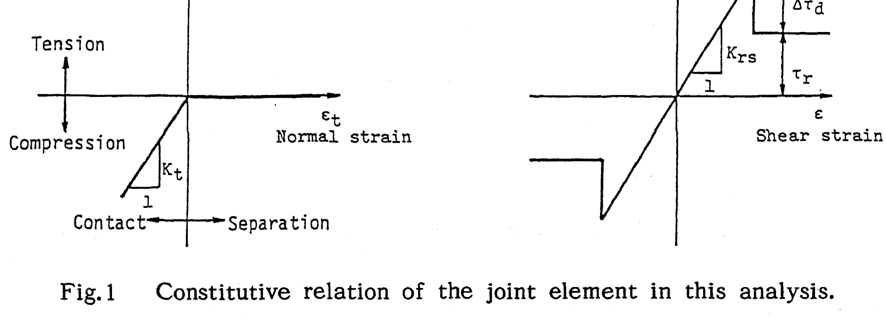

Fig.1 Constitutive relation of the joint element in this analysis.

The released strain energy is transformed into kinematic energy and transmitted as elastic waves to the neighboring region which, in turn, redistributes the stress field in the crust.

APPLICATION

We simulated the rupture process of a fault associated with the 1971 San Fernando earthquake; assuming a simple model. The finite element mesh of the model is shown in Fig.2. The dimensions of this model is 40 by 30 by 8km and these are 640 joint elements for the fault plane, 18,560 solid elements, 41x31x17=21,607 nodal points and a degree of freedom of 64,821. The structure of the crust is shown in Fig.3, and its physical properties are listed in Table 1. Rayleigh damping was assumed, and the Q value was set at 22.5 at 0.1Hz and at 200 at 1.0 Hz. The fault is a thrust type, with a potential rupture area (denoted by the dotted line) that is 40km long and 16km wide (Fig.4) and has a dip angle of 30 degrees. The dashed line shows the area considered in this analysis. Two strong motion accelerograph stations, at the Pacoima Dam (PAC) and at the Jet Propulsion Laboratory (JPL), are located within the area analyzed.

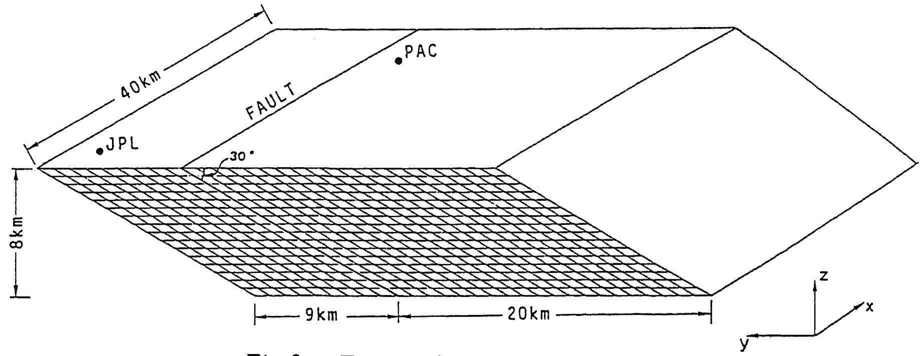

Fig.2 Finite element mesh.

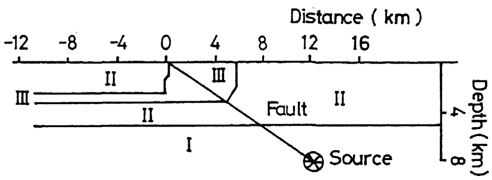

Fig.3 Configuration of the crust analyzed.

Table 1 Physical properties of the crust

Crust	Unit weight tf/m³	Vp km/s	Vs km/s	Poisson's ratio
I	3.0	6.0	3.4	0.27
II	2.5	6.0	3.4	0.24
III	2.7	4.2	2.5	0.22

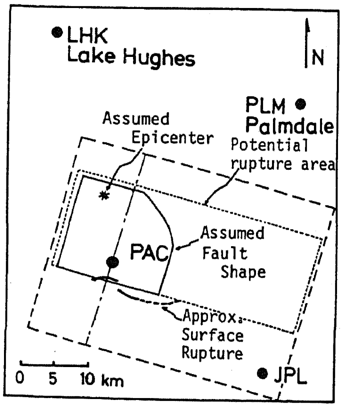

Fig.4 The region analyzed.

We adopted the distribution of stress drop reported for this earthquake by Jungles and Frazier(Ref.3). The distribution of the initial stress, the residual stress (defined as the difference between the initial stress and the stress drop) and the assumed yield stress are shown in Fig.5. These values are given for the region defined by the solid line in Fig.4, which is the fault plane determined by Heaton and Helmberger (Ref.4). This region corresponds to the right hand side of the fault plane shown in Fig.6. Outside of this region, a large yield stress value of 200 bars was given because

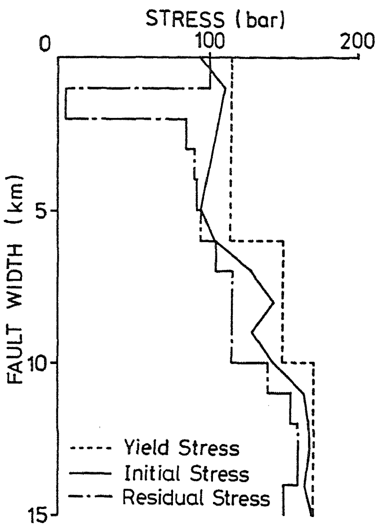

Fig.5 Distribution of the yield stress and the initial and residual stresses.

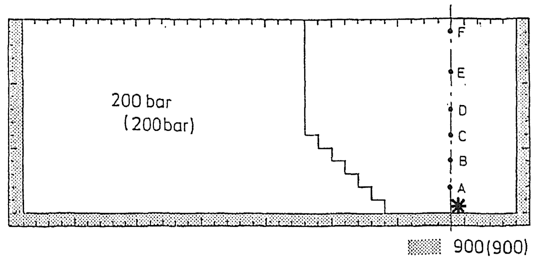

Fig.6 Potential fault plane.

significant rupture should not take palce (Fig.6). The fringe of the potential fault plane, which is shaded in Fig.6, should not have ruptured, therefore a higher yield stress level is given.

The rupture front is shown in Fig.7. Until 5 seconds after its initiation at the origin, rupture occured only in a narrow area because the stress drop over the region was low (Fig.5). Rupture developed within the region specified as layer I in Fig.3 until 9 seconds, thus it was transmitted horizontally because of the gap between the yield and initial stresses in region II. It behaved as a "barrier". After 9 seconds, its velocity increased rapidly and rupture reached the surface of ground within a few seconds. Propagation of the rupture stopped at about 14 seconds. The dashed line in Fig.7 defines the final ruptured zone which is broader than the area shown by the solid line in Fig.6. The source time function at points A to F on the fault plane in Fig.6 are given in Fig.8. The curves indicate that the rupture velocity varies at about 5, 9 and 14 seconds; the stoppage and abrupt growth of rupture being produced by the barrier effect.

We compared the time traces obtained by simulation with those recorded during the earthquake at the PAC and JPL stations. The acceleration, velocity and displacement curves of our simulation and the record are compared in Figs.9 (a)and(b); (a) is the PAC, N-S component and (b) the JPL U-D component. All the time traces were band-pass filtered between 0.07 and 2.0 Hz. Our comparison shows that the velocity and displacement curves are similar in shape and the significant phases of the corresponding time histories are easily identified (arrows). The peak value of the simulated waves at JPL, however, was smaller than the observed value, probably because the Q value assumed in our analysis is smaller than the real value of the crust. The average stress drop on the fault plane is 15 bars in our study, in which the value of Jungels and Frazier (Ref.3) was used; whereas, the value obtained by Kanamori and Anderson (Ref.5) is much larger for the same fault. This may be another reason for the low amplitude of the simulated ground motion.

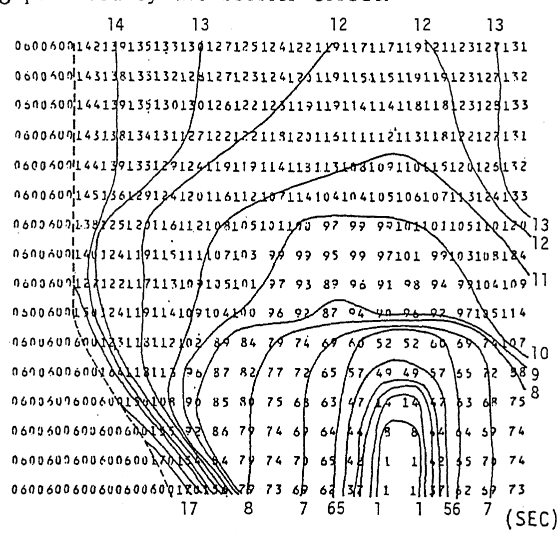

Fig.7 Rupture front.

Note that this simulation was done only once by relatively simple model and the parameters were not adjusted to obtain results that match the observed records. Performing a parameter survey under assumptions about such stress distributions as those of the initial, yield and residual stresses, enables us to determine the fault parameters of a past earthquake and to predict ground motion in the future (especially near-field ground motion), provided that there is reliable information to be analyzed on the stress distribution on the fault.

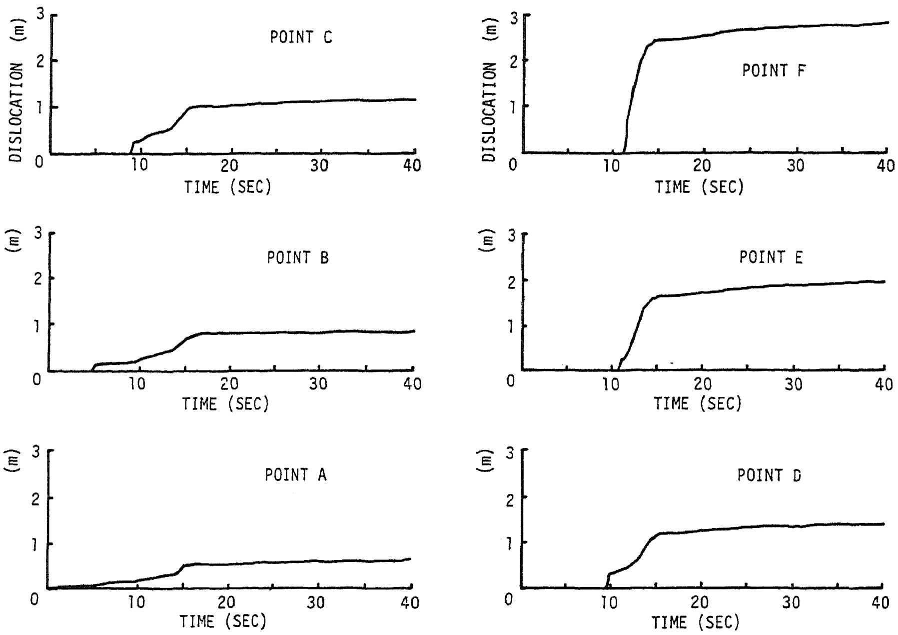

Fig.8 Source-time function at points A to F on the fault plane.

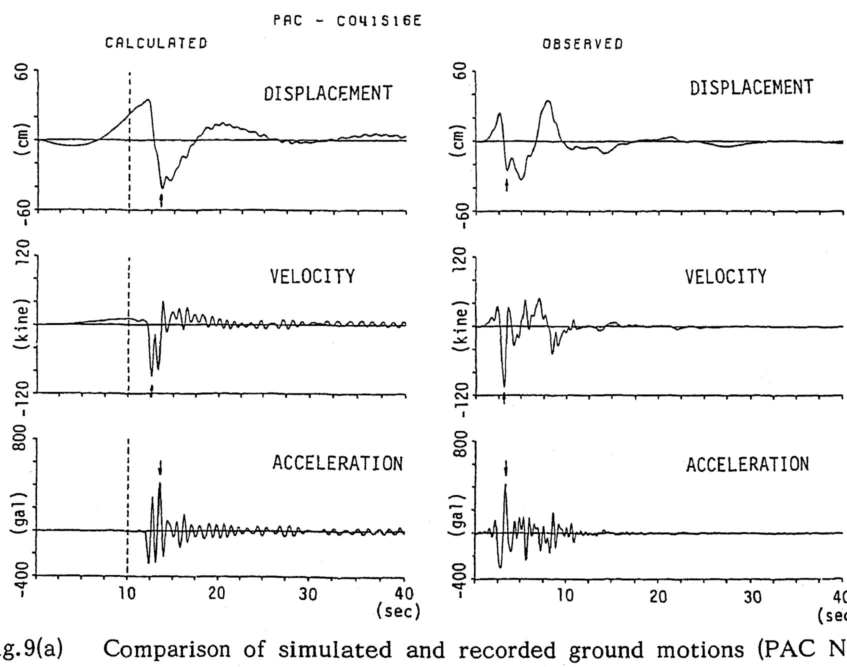

Fig.9(a) Comparison of simulated and recorded ground motions (PAC N-S).

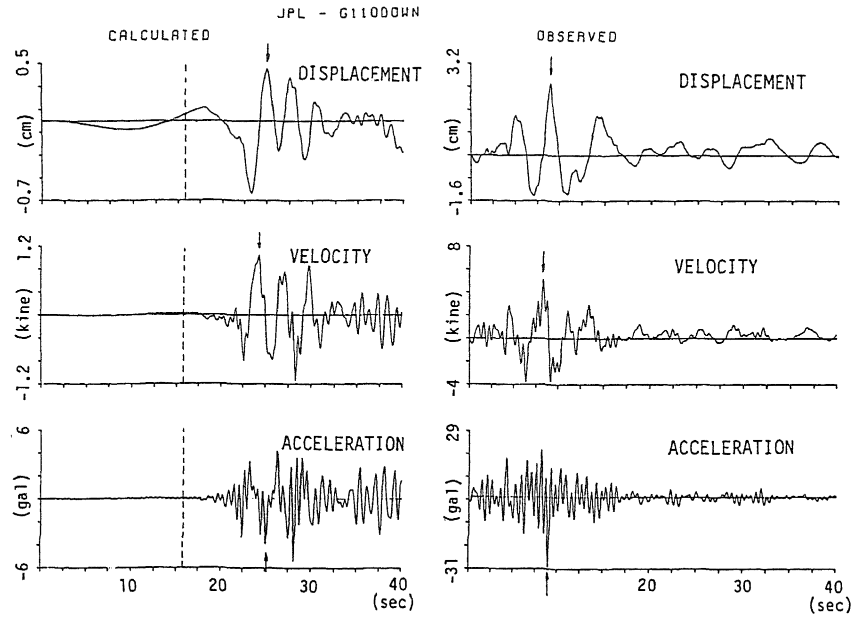

Fig.9(b) Comparison of simulated and recorded ground motions (JPL U-D).

CONCLUSION

We have developed a numerical technique that is suitable for dynamic analysis and this makes three-dimensional analysis possible. The ground motions computed by our method compare well with the strong motion accelerograms, integrated velocity and displacement curves recorded at the PAC and JPL stations during the 1971 San Fernando earthquake. This is evidence that our simulation method is able to model the rupture process, without assuming the fault parameters, provided a rough estimate of the strength parameters on the fault plane are given.

ACKNOWLEDGMENTS

We thank Dr. Fusanori Miura, Associate Professor of Yamaguchi University, for his useful advices on our research. This study was supported by a Grant-in-Aid for Research on National Disasters, from the Ministry of Education, Science and Culture of Japan.

REFERENCES

1. Toki, K., T. Sato and F. Miura: Separation and Sliding Between Soil and Structures During Strong Ground Motion, Earthquake Engineering and Structural Dynamics, Vol.9, pp.263-277, 1981.
2. Toki, K. and F. Miura: Simulation of a Fault Rupture Mechanism by a Two-Dimensional Finite Element Method, J. Phys. Earth, 33, pp.485-511, 1985.
3. Jungels, P. H. and G. A. Frazier: Finite Element Analysis of the Residual Displacements for an Earthquake Rupture: Source Parameters for the San Fernando Earthquake, J. of Geophys. Res., 23, pp.5062-5083, 1973.
4. Heaton, T. H. and D. V. Helmberger: Generalized Ray Model of San Fernando Earthquake, Bull. Seism. Soc. Am., vol.66, No.5, pp.1501, 1976.
5. Kanamori, H. and D. Anderson: Theoretical basis of some Empirical Relations in Seismology, Bull. Seism. Soc. Am., vol.65, No.5, pp.1073-1095, 1975.